Multi-elemental analysis of solidified mineral melt samples by laser-induced breakdown spectroscopy coupled with a linear multivariate calibration

Laville, Stéphane; Sabsabi, Mohammad; Doucet, François R.

Publisher's version / Version de l'éditeur:
https://doi.org/10.1016/j.sab.2007.10.003
Spectrochimica Acta Part B: Atomic Spectroscopy, 62, 12, pp. 1557-1566, 2007-10-17

ELSEVIER

Spectrochimica Acta Part B 62 (2007) 1557 – 1566

SPECTROCHIMICA ACTA PART B

www.elsevier.com/locate/sab

Multi-elemental analysis of solidified mineral melt samples by Laser-Induced Breakdown Spectroscopy coupled with a linear multivariate calibration ☆

Stéphane Laville *, Mohamad Sabsabi, François R. Doucet

National Research Council of Canada, Industrial Materials Institute, 75 de Mortagne Blvd., Boucherville, Québec, Canada J4B 6Y4

Received 20 December 2006; accepted 2 October 2007
Available online 17 October 2007

Abstract

Laser-Induced Breakdown Spectroscopy (LIBS) has been successfully applied for multi-elemental analysis of solidified mineral melt samples containing several oxides present in various concentrations. The plasma was generated using a Nd:YAG laser and the spectra were acquired using an Echelle spectrometer, coupled to an ICCD detector, which covers a spectral range from 200 to 780 nm. Using a set of 19 calibration samples, we first established univariate calibration curves for the major elements (Al, Fe, Mg, Ca, Ti and Si). We found out that the presence of matrix effects makes such a model, traditionally used in LIBS, not satisfying for quantitative analysis of such samples. Indeed, no sufficiently linear trends can be extracted from the calibration curves for the elements of interest considering all the samples. Instead, a much more robust calibration approach was obtained by considering a multivariate model. The matrix effects are then taken into account by correcting the spectroscopic signals emitted by a given species due the presence of the others ones. More specifically, we established here a calibration model using a 2nd order polynomial linear multivariate inverse regression. The capability of this approach was then checked using a 2nd set of samples with an unknown composition. A good agreement was observed between the analysis provided by X-ray fluorescence (XRF) and the LIBS measurements coupled to the multivariate model for the unknown samples.

Keywords: Laser-Induced Breakdown Spectroscopy; Glass analysis; Multivariate inverse calibration

1. Introduction

The glass producing industry faces the major challenge of increasing productivity to reduce cost and maximize the benefits from existing equipment. During refining, it is critical that operating parameters can be adjusted and controlled so that the chemistry of the melt is within predetermined limits. There is an increasing interest in technologies able to aid in the automation, quality and process control of the glass production processes. Techniques are sought for the continuous real-time monitoring of mineral melt composition and the various elements involved in the production of glass. The main chemical compounds present in the mineral melt are generally oxides such as SiO_2, Al_2O_3, Fe_2O_3, MgO, CaO, TiO_2, Na_2O, K_2O, P_2O_5 and MnO.

Presently, charge compositions in many industrial processes are monitored by periodic sampling followed by time-consuming sample preparation and laboratory analysis. The required steps for analysis by conventional techniques involve taking a sample from the melt, solidification of the sample, transport of the sample to a central laboratory, sample preparation and finally analysis, e.g., by conventional techniques such as atomic absorption spectroscopy (AAS) [1], X-ray fluorescence analysis (XRF) [2], inductively coupled plasma coupled to atomic emission spectroscopy (ICP-AES) spectroscopy [3], and ICP mass spectrometry (ICP-MS) [3]. These methods appear to be

☆ This paper was presented at the 4th International Conference on Laser Induced Plasma Spectroscopy and Applications (LIBS 2006) held in Montreal, Canada, 5–8 September 2006, and is published in the Special Issue of Spectrochimica Acta Part B, dedicated to that conference.

* Corresponding author. Tel.: +1 450 641 5230; fax: +1 450 641 5106.
E-mail addresses: stephane.laville@cnrc-nrc.gc.ca (S. Laville), Mohamad.sabsabi@cnrc-nrc.gc.ca (M. Sabsabi), francois.doucet@cnrc-nrc.gc.ca (F.R. Doucet).

0584-8547/$ - see front matter.
doi:10.1016/j.sab.2007.10.003

hampered in practice by their off line character. Virtually eliminating or shortening this delay through real-time in-situ Laser-Induced Breakdown Spectroscopy (LIBS) analysis has the potential to significantly increase productivity and improve process control. LIBS is a form of atomic emission spectroscopy based on plasma induced by focusing a laser beam on the sample. LIBS has features which make it useful tool for real-time measurements. This includes: multi-element analysis, non-contact measurements regardless of the material to be analyzed, high measuring speed, and no sample preparation or the preparation can be done by the laser beam itself.

LIBS investigations of glass were carried out by several groups [4–12]. In contrast to the analysis of metallic alloy, the analysis by LIBS of glass whether it is in the solid or liquid phase presents some difficulties due to the lack of major element for normalization and the large range of variation of the major or minor elements concentration. The influence of the wide ranges of analyte concentrations in glass samples poses a major problem for quantification. In fact, the line intensity of a given analyte element is not only affected by the concentration of that analyte but also with the variation of concentrations of other elements which is known in the literature by matrix effects. In these conditions the univariate approach, traditionally used in LIBS analysis, will not be appropriate since it provides values with large uncertainty and makes the LIBS measurement not reliable. Other chemometric alternatives should be used and further works need to be done in order to provide accurate and reliable measurements of the glass composition. The goal of the work presented here was to provide a method based on LIBS for the quantitative analysis of glass sample. The main issue to be solved here includes matrix effects due to the wide range of analyte concentrations. We would like to point out here that most of the LIBS literature was devoted to the analysis of minor or trace element, from a few ppm to a few %, in an approximately constant matrix. Very few works were devoted to the analysis of minor or major elements in a varying matrix. Furthermore, the use of chemometrics in LIBS analysis is still in its infancy by comparison to other conventional techniques based on near-infrared spectroscopy [13,14]. (More details about chemometrics can be found in [15] and [16].) To take into account the matrix effects, different chemometrics approaches, such as partial least square (PLS) [17,18] and principal components regression (PCR) [18–20] have been already used in LIBS. They are based on orthogonal projections of the LIBS spectral data for extracting the relevant information to feed the multivariate model therefore. However, several works have already shown that a simplest data selection can be used prior to the multivariate regression for steel [21,22], slag [23], aluminum [24] and even wood preservatives [25]. In this paper, the latter was also considered here due to the industrial context of this work.

2. Experimental

For this work, we disposed 19 solidified mineral melt samples which mainly contain the SiO_2, Al_2O_3, Fe_2O_3, MgO, CaO, TiO_2, Na_2O, K_2O, P_2O_5 and MnO oxides. These samples were directly taken from the mineral melt in a plant and were made by pouring a small amount of liquid glass into a platinum mold waiting until solidification. They were then machined by cutting a slice with a diamond saw in order to offer a flat surface to the laser. We show in Table 1 the composition of these samples, where the concentrations are given in % weight, characterized using the X-ray fluorescence (XRF) technique.

The experiments were carried out using a Q-switched Nd: YAG laser (Continuum, Surelite II) that can deliver up to 600 mJ/pulse at a wavelength of 1064 nm with a pulse duration of 7 ns FWHM and a maximum repetition of rate of 10 Hz. The

Table 1
Sample designation and composition

Designation	SiO_2	Al_2O_3	Fe_2O_3	MgO	CaO	TiO_2	Na_2O	K_2O	P_2O_5	MnO
1	41.8	19.9	6.9	7.7	19.2	1.5	1.3	0.8	0.4	<0.1
2	**62.6**	**4.4**	4.5	**25.0**	**1.3**	0.2	0.9	0.5	<**0.1**	<0.1
3	46.1	16.0	6.4	11.2	16.1	1.2	1.1	0.8	0.6	<0.1
4	55.4	6.9	2.0	12.8	20.9	0.5	**0.5**	0.6	0.1	<0.1
5	45.8	20.0	3.4	8.1	16.8	0.6	**3.5**	0.7	0.1	<0.1
6	**32.7**	15.5	5.7	14.4	27.8	1.2	1.1	0.7	0.3	<0.1
7	48.6	**31.6**	**1.2**	**0.4**	14.4	**0.1**	3.0	**0.2**	<**0.1**	<0.1
8	45.2	25.5	4.0	4.2	16.8	0.8	2.0	0.5	0.2	<0.1
9	39.3	21.4	3.2	9.1	22.8	0.7	1.6	0.5	0.8	<0.1
10	47.7	18.0	6.3	7.0	17.4	1.3	1.2	0.9	0.3	<0.1
11	44.7	23.7	5.0	5.4	17.7	1.0	1.8	0.6	0.3	<0.1
12	42.1	15.7	7.0	16.1	15.4	1.2	1.0	0.7	0.3	<0.1
13	35.8	16.9	5.6	6.7	**31.5**	1.1	1.0	0.7	0.3	<0.1
14	37.7	17.8	**15.7**	6.8	17.6	1.4	1.1	0.8	0.3	<0.1
15	39.7	18.8	11.2	7.3	18.5	1.4	1.2	0.8	0.3	<0.1
16	49.5	14.4	13.0	9.6	6.9	2.0	2.7	1.1	0.7	<0.1
17	45.7	17.0	9.9	8.7	13.1	1.7	2.0	1.0	0.5	<0.1
18	40.5	11.6	9.9	8.1	23.1	1.5	2.8	0.9	**1.8**	<0.1
19	46.8	19.1	6.7	5.2	13.5	**2.9**	**3.5**	**1.5**	0.3	<0.1

The concentrations are given in % weight.
The values in bold indicate the minimum and maximum concentrations for each chemical compound.

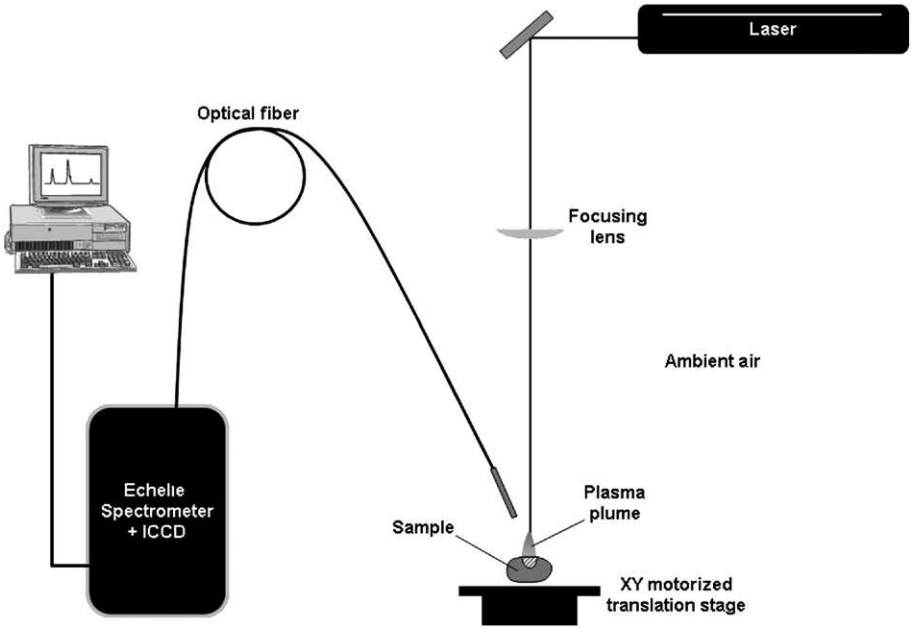

Fig. 1. Schematic experimental set-up with the Echelle spectrometer.

laser energy was set here to 100 mJ and the beam was focused onto the target using a plano-convex BK7 lens (25.4 mm diameter, focal length f=25 cm) perpendicularly to the target normal. In these conditions, the measured spot diameter onto the surface of the samples was 600 μm, which yields a laser fluence of about 35 J/cm^2. The ablation was experienced in air at atmospheric pressure. A schematic drawing of the experimental set-up is shown in Fig. 1.

The light emitted by the plasma was collected using a 1.5 m long, 600 μm core diameter optical fiber connected to the entrance of the spectrometer. A Czerny–Turner spectrometer appears not to be the best option here since it was too much time-consuming and did not offer a sufficient compromise between the observed spectral range and the spectral resolution. Indeed, the rich spectrum resulting from the strong presence of iron in the calibration samples requires the use of a high-resolution spectrograph to avoid spectral interferences. As a matter of fact, a typical 0.5 m focal length Czerny–Turner spectrometer equipped with a 2400 lines/mm grating gives a good resolution of about 0.03 nm. However, since the width of the spectral window (about 7 nm) should not be sufficient to observe all the elements simultaneously, several spectral windows must be considered. Consequently, we preferred using an Echelle spectrometer (ESA3000, LLA, Germany) coupled with an intensified CCD detector (Kodak KAF-1001, 1024×1024 pixels). This equipment offers a large spectral range, from 200 to 780 nm, while keeping a very high resolution, from 0.005 to 0.019 nm depending on the spectral region. (We point out here that spectra exhibit some gaps above the 580 nm due to the mismatch of the spectral orders and the size of CCD intensifier.) Therefore, the end of the optical fiber was connected to the entrance slit (35 μm width and 500 μm height) of the Echelle spectrometer.

The operating conditions consist here in a delay t_{delay}=4 μs and a gate width t_{int}=10 μs. Since for each laser pulse the total data processing with our spectrograph is about 4.2 s, we need to use a low repetition rate with the ablation laser, which was here 0.24 Hz (which corresponds to 1 shot every 4.2 s). The low repetition rate was a limitation dictated by the readout of the CCD detector. However, in our conditions, it has an advantage of reducing the fluctuations from shot to shot by decreasing the formation of aerosols in front of the target that deteriorates the reproducibility of measurement.

For this study, we limited our effort to the study of the major oxides which are, according to Table 1, SiO_2, Al_2O_3, Fe_2O_3, MgO, CaO and TiO_2. Actually, it appeared that no suitable lines were found for the other oxides, Na_2O, K_2O and P_2O_5 in our experimental conditions. Indeed, this is due to the low concentrations of these elements in the samples and the low sensitivity of the ICCD detector/Echelle spectrograph in the spectral regions where these elements emit the most intensively (UV region and/or in the red region of the spectrum). In addition, MnO was not considered in our model due to its very low concentration (less than 0.1% — see Table 1). The selected spectral lines used for the calibration of the elements of interest are presented in Table 2.

These lines were chosen suitably in order to minimize spectral interferences and self-absorption. In addition, the intensity of these lines was supposed to vary linearly with the concentration within the range of concentration for all the

Table 2
Spectral lines used for the calibration

Elements of interest	Calibration lines	E_i (cm^{-1})	E_j (cm^{-1})	A_{ji} (s^{-1})
Al	Al(I) 265.249 nm	0	37,689.41	0.13
Fe	Fe(I) 404.582 nm	11,976.23	36,686.16	0.86
Mg	Mg(I) 383.829 nm	21,911.18	47,957.03	0.38
Ca	Ca(I) 585.746 nm	23,652.30	40,719.85	0.66
Ti	Ti(II) 337.280 nm	94.10	29,734.54	1.1
Si	Si(I) 390.553 nm	15,394.37	40,991.88	0.12

samples considered in this paper. It is also important to mention here that we assumed that all the oxide molecules are dissociated into the plasma in order to be able to assimilate the atomic concentration as the oxide one. This is generally the case for LIBS plasmas due to the high temperatures, typically some electron-volts initially.

In Fig. 2, we show a selected, ranging from 382 to 391 nm, region of the Echelle spectrum obtained with the samples denoted 2 and 9. Specifically, the Mg(I) 383.829 nm and the Si (I) 390.553 nm lines used for the calibrations are observed in this window. This LIBS spectrum confirms that there is more SiO_2 and MgO in sample 2 (62.6% SiO_2 and 25% MgO) than in sample 9 (32.7% SiO_2 and 14.4% MgO) as shown in Table 2. The high resolution of the Echelle spectrometer is also well demonstrated in Fig. 2.

Therefore, for each sample, in order to get a representative sampling, and account for any eventual spatial inhomogeneity, we acquired 10 spectra at each of the 25 positions of a 5×5 matrix with a 1 mm intersite distance. At each position, the experimental procedure consisted firstly in firing 100 cleaning shots, at a repetition rate of 3 pulses/s, in order to avoid detecting contaminations at the surface of the samples. Therefore, we acquired the spectra corresponding to the subsequent 10 shots. The samples were automatically translated during the LIBS measurements using a double axis motorized stage (Newport, UTM 100 mm) controlled by a programmable controller (Newport, model ESP 300). The repetition accuracy of translation is about 1 μm.

3. Results and discussion

3.1. Calibration curves

3.1.1. Normalized univariate regression

Based on the spectra acquired using the Echelle spectrograph using our set of calibration samples (see Table 1 for their composition), we first performed a univariate calibration for the selected lines shown in Table 2. In order to minimize the signal variations due to laser energy fluctuations and to random changes in plasma position relative to the collection optics, it is preferable to normalize, spectrum to spectrum, the signals of the elements of interest. In this study, the internal standardization is achieved using the Si(I) 390.553 nm line. The choice of this line is mainly guided by the fact that its variations over the concentration of SiO_2 appear to be relatively weak for our batch of samples: from 32.7% (sample 6) to 62.6% (sample 2). On the contrary, the concentrations of the other elements are too disparate to be reliable.

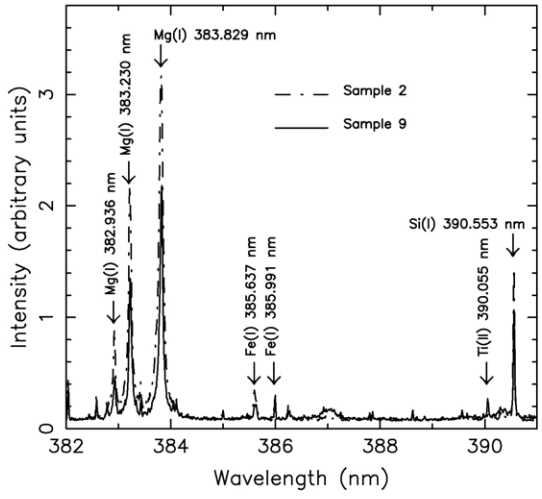

Fig. 2. Illustration of a region of a single laser shot spectrum obtained with the Echelle spectrometer for glass samples denoted 2 and 9.

We present on Fig. 3a–e the intensity of the elements of interest normalized by the signal of Si(I) 390.553 nm as a function of the concentration ratio, obtained with the 19 calibration samples. The vertical error bars on each data point indicate the fluctuations, from shot to shot, between the 250 shots performed on each sample. They can be attributed to slight inhomogeneity of the samples and the LIBS technique itself through fluctuations of the laser energy and the collection of light. In addition, it is also well known that the reproducibility of an Echelle spectrometer can be strongly affected by fluctuations of the ambient temperature. Indeed, the index of refraction of the separating-orders prism into the Echelle spectrometer is very sensitive with the temperature, so the position of the optical image on the CCD, called the Echellogram. The relatively small experimental error bars indicate that we can provide a reasonable reproducibility of the measurements using the LIBS technique in these conditions.

Taking into account the error bars, it clearly appears from Fig. 3 that there is no evidence of linear trend between the intensity ratios and the concentration ratios, considering all the samples. This behavior has already been observed experimentally by S. Palanco et al. [21] while establishing a calibration curve for iron using a set of stainless-steel samples. Indeed, they found out a poor correlation, $R^2=0.3371$, between the Fe(I) 358.119 nm line intensity and the iron concentration. However, for Al_2O_3, Fe_2O_3 and MgO oxides, we can reasonably extract linear tendencies from Fig. 3 eliminating a few samples.

3.1.2. Normalized multivariate regression

We showed that a univariate calibration is not enough satisfying here due to the presence of significant matrix effects in the spectroscopic signals with our samples. However, in atomic emission spectroscopy techniques, such a limitation can be generally reduced using mathematical post-processing procedures based on chemometrics. It consists basically in taking into account, for the signal for a given element, the signals of the other major elements present into the matrix. The goal of such approaches is mainly to improve the precision and the accuracy on the LIBS measurements when compared with a prediction based on a univariate calibration.

In [21], it is shown that the influence of the matrix effects in LIBS can be reduced using a linear multivariate regression for steel samples. Indeed, for most of the elements (Fe, Cr, Ni, Cu and Ti) present in the sample, the coefficient of determination R^2 of the corrected calibration curves was higher than 0.98. In [22], a partial least square (PLS) regression model was used to perform quantitative analyses by LIBS of preservatives on

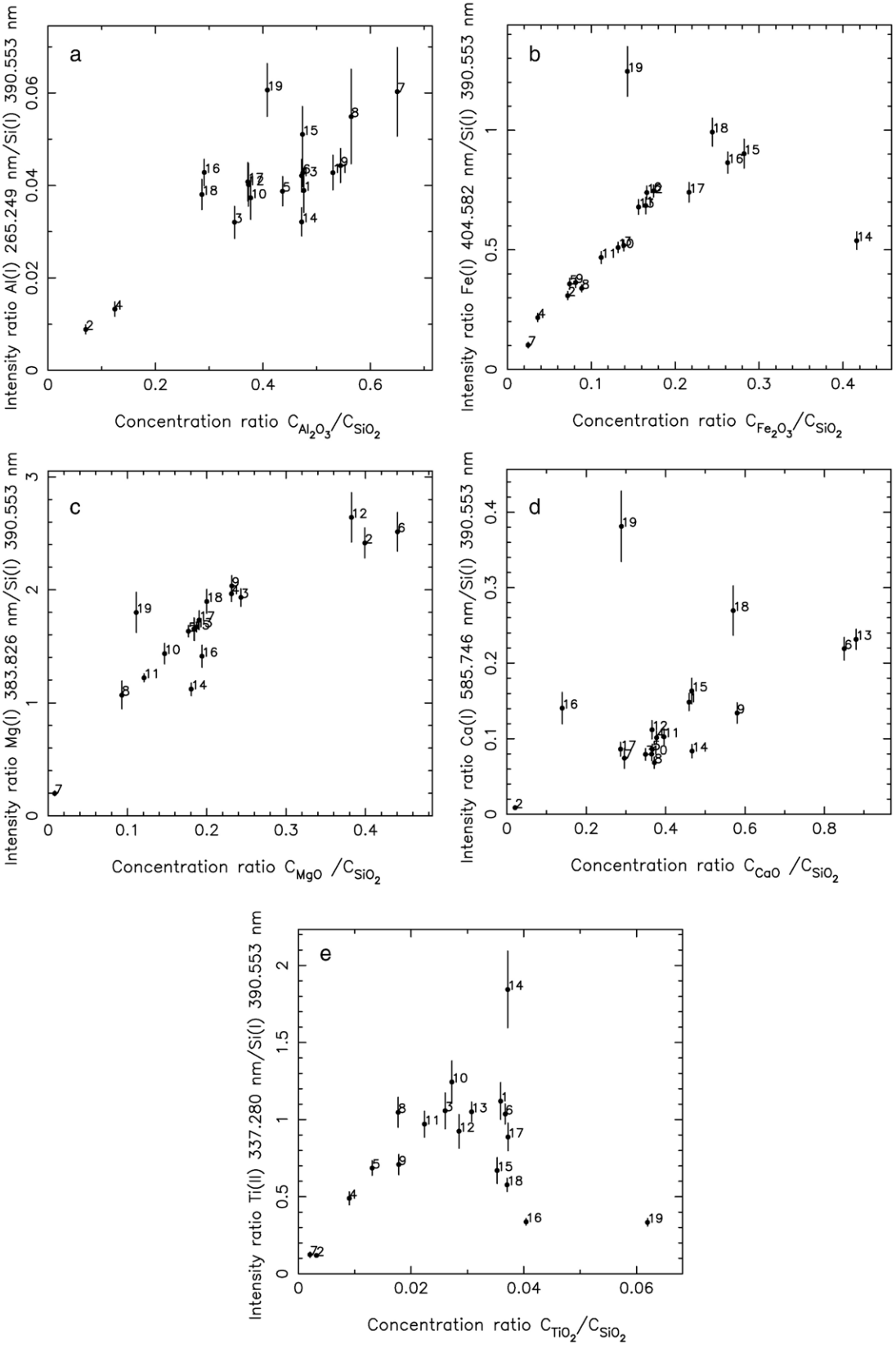

Fig. 3. Univariate calibration curves for the selected spectral line normalized by the Si(I) 390.553 nm line: (a) Al(I) 265.249 nm, (b) Fe(I) 404.582 nm, (c) Mg(I) 383.826 nm, (d) Ca(I) 585.746 nm and (e) Ti(II) 337.280 nm.

treated woods. The Cu, As, Zn and Cr concentrations predicted by LIBS were in good agreement with the ones measured with a standard technique. Finally, in [23], analysis of Fe, Ca and Si in slag samples from a steel plant using LIBS provided better results when combined with a multivariate approach instead a of a univariate approach.

In this paper where LIBS was applied on solidified glass samples exhibiting complex matrices, a 2nd order polynomial multivariate inverse regression was considered. This approach is similar to the linear multivariate model described in [21] but light departure from linear correlation between spectroscopic signals and light self-absorption effects can be also modeled. We give in the following a detailed overview about the mathematical treatment and its physical interpretation in the case of optical spectroscopy.

If we designate by n the number of samples used to establish the calibration and m the number of components of interest (m is also the number of emission lines). For a given component labeled by j (where $1 \le j \le m$), the linear multivariate inverse regression method limited to the 2nd order consists simply in writing:

$$[C_j] = b_{0,j} + \sum_{i=1}^{m} \left(b_{i,j}[I_i] + b_{m+i,j}[I_i]^2 \right) + [e_j] \quad (1)$$

where $[C_j]$ is the vector of net (or normalized) concentration of the jth component, the coefficients $b_{i,j}$ are known as the parameters of the non-linear multivariate regression, $[I_i]$ is the vector of the net (or normalized) line intensities of the ith component, and finally $[e_j]$ is the vector of the residuals which corresponds basically to the discrepancies between the prediction given by the multivariate regression model and the linear regression obtained with the multivariate results. The dimension of these three vectors is n. A simplified approach consists in writing Eq. (1) in the following matrix form:

$$[C_j] = [U][B_j] + [e_j] \quad (2)$$

where

$$U = \begin{pmatrix} 1 & I_{1,1} & \dots & I_{1,m} & (I_{1,1})^2 & \dots & (I_{1,m})^2 \\ 1 & I_{2,1} & \dots & I_{2,m} & (I_{2,1})^2 & \dots & (I_{2,m})^2 \\ \dots & \dots & \dots & \dots & \dots & \dots & \dots \\ 1 & I_{n,1} & \dots & I_{n,m} & (I_{n,1})^2 & \dots & (I_{n,m})^2 \end{pmatrix}$$

is a matrix of dimensions $n \times (2m+1)$ containing only the spectroscopic signals and

$$B = \begin{pmatrix} b_{0,j} \\ b_{1,j} \\ \dots \\ b_{2n,j} \end{pmatrix}$$

is a vector containing the unknown parameters of the regression model. The 11 unknowns, from $b_{0,j}$ to $b_{2n,j}$, of this system are then obtained by minimizing the quantity $\chi_j^2 = \sum_{i=1}^{n} e_{i,j}^2$ usually called predicted residual sum of squares (PRESS) [15]. The vector of the concentrations predicted by the multivariate model is then given by Eq. (3):

$$[\hat{C}_j] = [C_j] - [e_j] = [U][B_j]. \quad (3)$$

To establish the regression model, the procedure consists firstly in calculating the signal matrix $[U]$ and the concentration ratios $[C_j]$ matrix. Therefore, since the U matrix is not square, the pseudo-inverse [15] is used to calculate the predicted concentration ratios:

$$[\hat{C}_j] = P[C_j] \quad (4)$$

where $P = U(U^T U)^{-1} U^T$ is a projection matrix, U^T designates the transpose of U and U^{-1} designates the inverse of U. Finally, the residuals $[e_j]$ are calculated from Eq. (3).

Establishing a reliable calibration model requires generally taking into account all the compounds present into the samples. However, according to Table 1, we did not take in to account the contribution of Na_2O, K_2O, P_2O_5, and MnO in the model. Indeed, the appropriate analytical lines for these elements, which are suitable and free from interference for the range of concentrations in our conditions, are in the red region (for K and Na) or in the far UV (P) where the sensibility of our detection system Echelle/ICCD is rather very poor. Furthermore, these oxides represent together less than 5% of the composition in percents weight. Consequently, a multivariate analysis was applied to our data using the signals of Al, Fe, Mg, Ca and Ti normalized by the signal of Si and the concentration ratios, normalized to concentration of SiO_2, was also considered. In our model, we computed $n=19$ calibration samples (see Table 1) and $m=5$ intensity ratios. It is also worth mentioning here that mathematically there is a minimum number of standard samples required to establish this calibration model. Indeed, strictly speaking, it should be minimally equal to the number of elements plus one. However, in order to improve the quality of the regression, it should be preferable to use saying at least about two times the minimum number of samples required. This means that for the 2nd order non-linear model, we should compute at least $2(2n+1)$, which means 22 here, calibration samples. Even if only 19 samples were available for this work, we are quite confident that this was enough since they were rather representative of the most common glass samples. Actually, we will stress this issue thereafter by providing the capability of prediction of composition of unknown samples when compared to XRF measurements.

Since we have neglected the presence of K_2O, P_2O_5, Na_2O and MnO in our samples, the other oxide concentrations, given in % weight, verify the condition $C_{SiO_2} + C_{Al_2O_3} + C_{Fe_2O_3} + C_{MgO} + C_{CaO} + C_{TiO_2} \approx 1$. From this equation, the SiO_2 concentration can be easily deduced and therefore the individual concentrations of the other oxides.

We present in Fig. 4a–c the concentrations of three selected oxides, Fe_2O_3, CaO and TiO_2, predicted by LIBS combined with our linear multivariate model for our 19 calibration samples as a function of their concentrations measured by XRF.

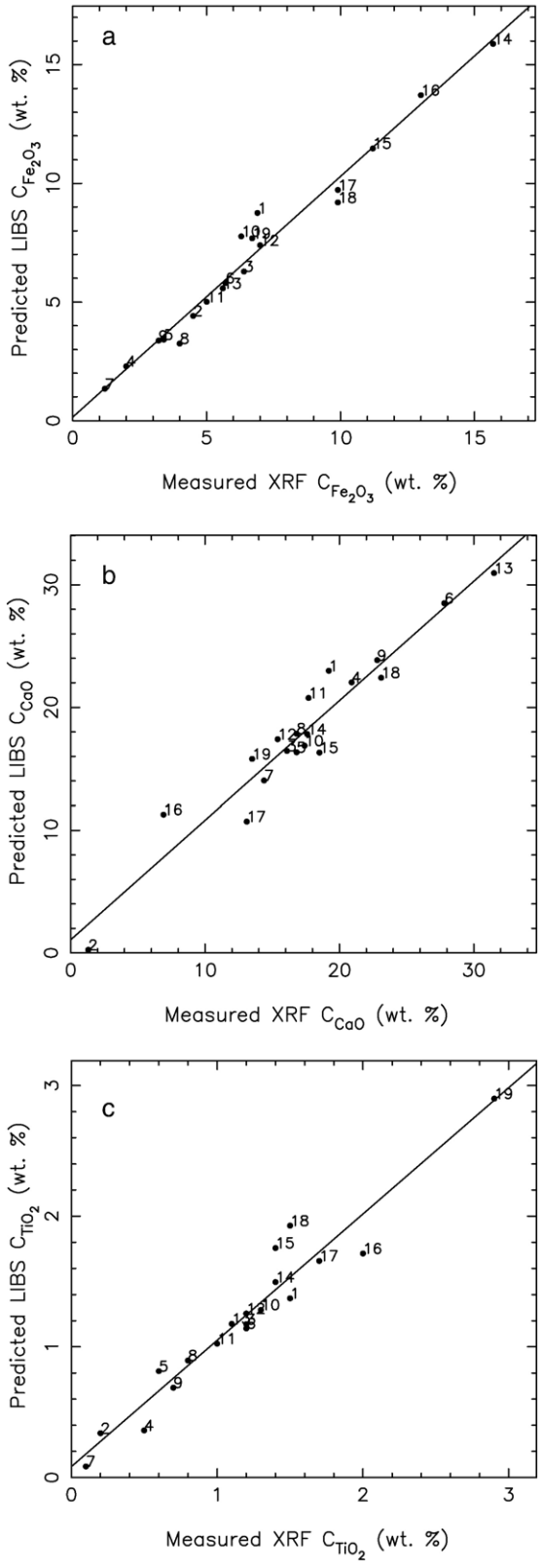

Fig. 4. Concentrations (in % weight) of Fe_2O_3 (a), CaO (b) and TiO_2 (c) predicted by LIBS as a function of the concentrations measured by XRF for the calibration samples.

(Graphs obtained for Al_2O_3, MgO and SiO_2 exhibits a very similar behavior but are not shown here.)

In Table 3, we present the coefficient of determination R^2, the relative standard error (RSD) and the root-mean-square error of calibration (RMSEC) associated to the linear regression performed on the data shown on Fig. 4. ($RMSEC^2$ is defined by the ratio of the PRESS calculated for the calibration samples by the number of degrees of freedom which is here $n-1$.) The quantities R^2 and RMSEC indicate the quality of the multivariate model while the RSD corresponds to the systematic error associated to the R^2 coefficient. As shown in Table 3, our multivariate regression model provides R^2 values higher than 0.92 for all the elements of interest here. This indicates that a reasonable correlation is obtained for the calibration samples. The global error on the prediction curves shown in Fig. 4 is the sum of three contributions. The first one is due to regression model itself and is characterized by the relative standard error (RSD) shown in Table 3. Another one is the uncertainties on the concentrations measured by XRF, which can be estimated to about a few percents on the measured values. Finally, the LIBS technique itself introduced also an uncertainty on the spectroscopic signals as already mentioned in Section 2.

3.2. Validation of the model

Finally, as a validation of the calibration model, we predicted the composition of 12 solidified mineral melt samples, denoted 20 to 31, with unknown composition.

In Fig. 5a–c, we present a comparison of the concentration (in % weight) of the oxides selected on Fig. 4 for the unknown samples predicted using the LIBS combined with our multivariate model and those measured by X-ray fluorescence (XRF). We also indicated the expected error bars on the concentration of these various elements. This error is basically due to the systematic error on the multivariate regression (see Table 3) and the uncertainty on the intensity ratio for each line. We estimated the uncertainty on the mean intensity ratio, i.e., the repeatability of the measurement, to be generally about 3% in our conditions. We would like to point out here that these values give only an estimate of the error on the predicted concentration. We think that these errors are generally over-

Table 3
Coefficient of determination and RSDs for the prediction given by the multivariate regression model based on the 19 calibration samples

Element	Calibration samples			Prediction samples		
	R^2	RSD (%)	RMSEC (% weight)	R^2	RSD (%)	RMSEP (% weight)
Al	0.9573	7.13	1.45	0.9978	6.40	1.40
Fe	0.9727	9.18	0.69	0.9826	16.87	1.36
Mg	0.9840	7.29	0.76	0.9815	8.53	1.06
Ca	0.9256	10.24	1.96	0.9827	7.25	0.88
Ti	0.9353	13.57	0.17	0.9746	11.99	0.17
Si	0.9343	3.88	2.37	0.9999	4.10	2.08

RSD: relative standard deviation of the regression.
RMSEC: root-mean-square error of calibration.
RMSEP: root-mean-square error of prediction.

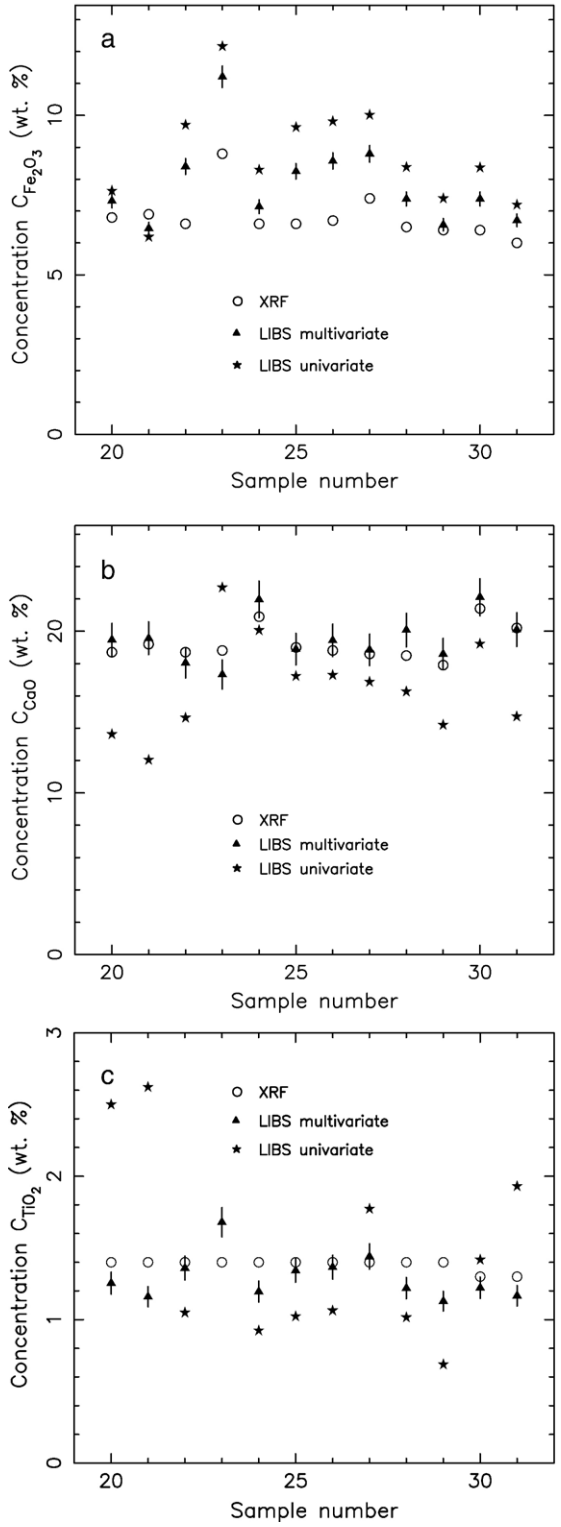

Fig. 5. Concentration (in % weight) of Fe_2O_3 (a), CaO (b) and TiO_2 (c) obtained measured by LIBS (combined with a univariate or a multivariate model) and XRF in the unknown glass samples.

estimated, except for samples with composition very different from the ones computed in the calibration model.

In Table 3, the values of the coefficient of determination R^2, the relative standard error (RSD) and the root-mean-square error of prediction (RMSEP) are shown for the validation samples. ($RMSEP^2$ is defined by the ratio of the PRESS calculated for the prediction samples by the number of prediction samples.) The correlation obtained for the prediction samples is very strong, R^2 higher than 0.97. It also appears that RMSEC is generally comparable to RMSEP.

Table 4
Minimum relative difference, maximum relative difference and mean relative difference between the values of concentration obtained by XRF and LIBS combined with a univariate or a multivariate calibration model (in bold)

Component	Al_2O_3	Fe_2O_3	MgO
Minimum relative difference (%)	**0.5 (sample 29)** 1.5 (sample 20)	**2.6 (sample 29)** 10.9 (sample 21)	**0.4 (sample 30)** 0.5 (sample 25)
Maximum relative difference (%)	**12.7 (sample 25)** 11.3 (sample 26)	**24.5 (sample 26)** 38.0 (sample 22)	**24.6 (sample 26)** 22.2 (sample 26)
Mean relative difference (%)	**5.6** 6.2	**14.5** 25.4	**10.1** 10.3
Component	CaO	TiO_2	SiO_2
Minimum relative difference (%)	**0.5 (sample 31)** 4.1 (sample 24)	**2.5 (sample 26)** 8.6 (sample 30)	**0.2 (sample 26)** 0.9 (sample 26)
Maximum relative difference (%)	**8.2 (sample 23)** 45.9 (sample 21)	**21.5 (sample 29)** 206.7 (sample 23)	**8.2 (sample 25)** 15 (sample 21)
Mean relative difference (%)	**3.6** 19.2	**10.7** 51.9	**4.0** 8.2

The sample number associated to the value is indicated between brackets.

Taking into account of the errors bars, Fig. 5 indicates that we obtained a good agreement between the values obtained by LIBS combined with a multivariate model and the XRF measurements. However, the concentration of Fe is slightly over-estimated. Actually, a more realistic model will require taking into all the compounds present in the samples.

Therefore, we present in Table 4 the minimum relative difference, the maximum relative difference and also the mean relative difference between the values of concentration obtained by LIBS combined with a univariate or a multivariate

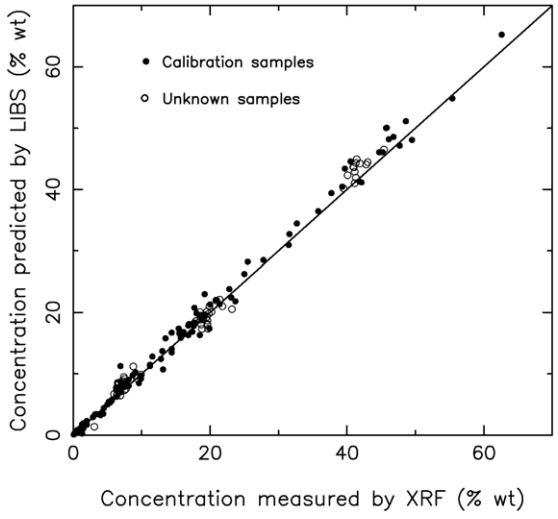

Fig. 6. Comparison between LIBS (coupled with a multivariate model) and XRF measurements obtained for the main oxides (SiO_2, Al_2O_3, Fe_2O_3, MgO, CaO and TiO_2) present in the 32 glass samples. The solid line corresponds to the perfect agreement between XRF and LIBS.

model and XRF. The results are presented for each main compound in the unknown samples and taken into account in our calibration model. The mean relative difference (given in %) was defined as: $\Delta_i = 100|C_i^{XRF} - C_i^{LIBS}|/\overline{C}_i$ where $\overline{C}_i = \left(C_i^{XRF} + C_i^{LIBS}\right)/2$.

Fig. 6 summarizes the results presented in this paper by showing the concentration obtained by LIBS combined with a non-linear multivariate model as a function of the XRF measurements for the two sets of samples, 19 calibration samples and 12 unknown samples, available for this work. The coefficient of determination of the global prediction curve shown in Fig. 6 is equal to $R^2 = 0.9989$, which indicates a good quality of the regression.

4. Conclusion

The goal of this work was to evaluate the potential of the Laser-Induced Breakdown Spectroscopy (LIBS) technique for multi-elemental analysis of solidified mineral melt samples. These samples contain several components among which the major ones are Al_2O_3, Fe_2O_3, MgO, CaO, TiO_2 and SiO_2.

The experimental results obtained here showed that the univariate calibration approach traditionally used in LIBS does not provide satisfactory results and is not reliable enough due to the presence of strong matrix effects. Instead, we found out that a 2nd order polynomial linear inverse multivariate regression model was a more satisfying approach. Indeed, the poor linearity of the univariate calibration curves can strongly affect the accuracy and the precision of the prediction. We showed here that the multivariate approach generally provides better predictions that the univariate approach, when compared with XRF measurements.

The results presented clearly show that the LIBS technique present a great potential for mineral melt, but must be combined to a multivariate model to provide accurate measurements. In principle, such an approach can be applied to the analysis of materials with wide range of analyte concentration and where matrix effects are an important issue. This kind of calibration approach is useful for quantitative analysis and clearly opens new field of applications for LIBS analysis of complex matrices.

Further improvements in the prediction of unknown samples are expected by computing a larger number of calibration samples into our multivariate model. We also believe that the results presented here could be improved using an Echelle spectrometer/detector exhibiting better performance. Furthermore, adding into the calibration model the presence of the other minor oxides, K_2O, P_2O_5, MnO and Na_2O, is expected to improve the accuracy of prediction. However, this improvement will require more calibration samples. Finally, further work needs to be addressed in order to apply this study for industrial on-line chemical analysis in the mineral melt for simultaneous analysis of multiple constituents.

Acknowledgments

The authors would like to thank Dr. Daniel Levesque from the Industrial Materials Institute (National Research Council of Canada, Boucherville) for the helpful discussions about the multivariate calibration and André Hamel for the technical support during the experiments.

References

[1] A.F. Lagalante, Atomic absorption spectroscopy: a tutorial review, Appl. Spectrosc. Rev. 34 (1999) 173–189.
[2] R. Jenkins, in: R.A. Meyers (Ed.), X-ray Techniques: Overview, Encyclopedia of Analytical Chemistry, J. Wiley & Sons Ltd, Chichester, 2000, pp. 13269–13288.
[3] A. Montaser, D.W. Golightly, Inductively Coupled Plasmas in Analytical Atomic Spectrometry, VCH Publishers, New York, 1992.
[4] U. Panne, C. Haisch, M. Clara, R. Niessner, Analysis of glass and glass melts during the vitrification process of fly and bottom ashes by laser-induced plasma spectroscopy. Part I. Normalization and plasma diagnostics, Spectrochim. Acta Part B 53 (1998) 1957–1968.
[5] U. Panne, M. Clara, C. Haisch, R. Niessner, Analysis of glass and glass melts during the vitrification of fly and bottom ashes by laser-induced plasma spectroscopy. Part II. Process analysis, Spectrochim. Acta Part B 53 (1998) 1969–1981.
[6] N. Carmona, M. Oujja, E. Rebollar, H. Römich, M. Castillejo, Analysis of corroded glasses by laser induced breakdown spectroscopy, Spectrochim. Acta Part B 60 (2005) 1155–1162.
[7] K. Loebe, A. Uhl, H. Lucht, Microanalysis of tool steel and glass with laser-induced breakdown spectroscopy, Appl. Opt. 42 (2003) 6166–6173.
[8] M. Ducreux-Zappa, J.-M. Mermet, Analysis of glass by UV laser ablation inductively coupled plasma atomic emission spectrometry. Part 2. Analytical figures of merit, Spectrochim. Acta Part B 53 (1996) 333–341.
[9] O. Schalm, D. Caluwé, H. Wouters, K. Janssens, F. Verhaeghe, M. Pieters, Chemical composition and deterioration of glass excavated in the 15th–16th century fishermen town of Raversijde (Belgium), Spectrochim. Acta Part B 59 (2004) 1647–1656.
[10] J.-I. Yun, R. Klenze, J.I. Kim, Laser-induced breakdown spectroscopy for the on-line multielement analysis of highly radioactive glass melt. Part I: characterization and evaluation of the method, Appl. Spectrosc. 56 (2002) 437–448.
[11] J.-I. Yun, R. Klenze, J.I. Kim, Laser-induced breakdown spectroscopy for the on-line multielement analysis of highly radioactive glass melt simulants. Part II: analyses of molten glass samples, Appl. Spectrosc. 56 (2002) 852–858.
[12] U. Panne, R.E. Neuhauser, C. Haish, H. Fink, N. Niessner, Remote analysis of a mineral melt by laser-induced plasma spectroscopy, Appl. Spectrosc. 56 (2002) 375–380.
[13] C.A. Watson, Near infrared reflectance spectrophotometric analysis of agricultural products, Anal. Chem. 49 (1977) 835A–840A.
[14] J. Worman Jr., A brief review of near infrared in petroleum product analysis, J. Near Infrared Spectrosc. 4 (1996) 69–74.
[15] H. Martens, T. Naes, Multivariate Calibration, John Wiley and Sons, New York, 1998.
[16] P. Geladi, Chemometrics in spectroscopy: part I. Classical chemometrics, Spectrochim. Acta Part B 58 (2003) 767–782.
[17] J. Amador-Hernandez, L.E. Garcia-Ayuso, J.M. Fernandez-Romero, M.D. Luque de Castro, Partial least squares regression for problem solving in precious metal analysis by laser induced breakdown spectrometry, J. Anal. At. Spectrom. 15 (2000) 587–593.
[18] H. Fink, U. Panne, R. Niessner, Process analysis of recycled thermoplasts from consumer electronics by laser-induced plasma spectroscopy, Anal. Chem. 74 (2002) 4334–4342.
[19] S.R. Goode, S.L. Morgan, R. Hoskins, A. Oxsher, Identifying alloys by laser-induced breakdown spectroscopy with a time-resolved high resolution Echelle spectrometer, J. Anal. At. Spectrom. 15 (2000) 1133–1138.
[20] J.B. Sirven, B. Bousquet, L. Canioni, L. Sarger, S. Tellier, M. Potin-Gautier, I.L. Hecho, Qualitative and quantitative investigation of chromium-polluted soils by laser-induced breakdown spectroscopy combined with neural networks analysis, Anal. Bioanal. Chem. 385 (2006) 256–262.

[21] S. Palanco, J.J. Laserna, Full automation of a laser-induced breakdown spectrometer for quality assessment in the steel industry with sample handling, surface preparation and quantitative analysis capabilities, J. Anal. At. Spectrom. 15 (2000) 1321–1327.
[22] J. Vrenegor, R. Noll, V. Sturm, Investigation of matrix effects in laser-induced breakdown spectroscopy plasmas of high-alloy steel for matrix and minor elements, Spectrochim. Acta Part B 60 (2005) 1083–1091.
[23] M. Kraushaar, R. Noll, H.-U. Schmitz, Slag analysis with laser-induced breakdown spectroscopy, Appl. Spectrosc. 57 (2003) 1282–1287.
[24] F.R. Doucet, T.F. Belliveau, J.-L. Fortier, J. Hubert, Use of chemometrics and laser-induced breakdown spectroscopy for quantitative analysis of major and minor elements in aluminum alloys, Appl. Spectrosc. 61 (3) (2007) 327–332.
[25] M.Z. Martin, N. Labbé, T.G. Rials, S.D. Wullschleger, Analysis of preservative-treated wood by multivariate analysis of laser-induced breakdown spectroscopy spectra, Spectrochim. Acta Part B 60 (2005) 1179–1185.